J Mater Sci: Mater Med (2008) 19:817–826
DOI 10.1007/s10856-007-3080-z

Tissue spinal cord response in rats after implants of polypyrrole and polyethylene glycol obtained by plasma

Roberto Olayo · Camilo Ríos · Hermelinda Salgado-Ceballos · Guillermo Jesus Cruz · Juan Morales · Maria Guadalupe Olayo · Mireya Alcaraz-Zubeldia · Ana Laura Alvarez · Rodrigo Mondragon · Axayacatl Morales · Araceli Diaz-Ruiz

Received: 5 June 2006 / Accepted: 5 April 2007 / Published online: 1 August 2007

Abstract Most of the biomaterials used nowadays for the reconstruction of the spinal cord (SC) tissue after an injury, tested in animals, have obtained modest results. This work presents a study about the compatibility of two novel, non-biodegradable, semi-conductive materials, obtained by plasma polymerization: iodine-doped pyrrole (PPy/I) and pyrrole-polyethylene glycol (PPy/PEG). Both polymers, separately, were implanted in the SC tissue of rats after a transection. Prior to implantation, the elemental composition and the physico-chemical properties of polymers were studied by electron scanning microscopy, IR Spectroscopy and thermogravimetric analysis. We used adult female Long Evans rats, subjected to SC transection. Animals were randomized to be allocated in one of the treatment groups and were killed four weeks after the lesion for histology study. Results showed that both implants were integrated to the SC tissue, as inflammatory and gliotic responses, similar to those observed in the control group, and rejection of the implant, were not evident. Moreover, the immediate effect of PPy/I or PPy/PEG in the injured SC prevented secondary tissue destruction, as compared to non-implanted control animals. In conclusion, implants of semi-conductive polymers were well-tolerated and integrated favorably to SC tissue after transection

R. Olayo · J. Morales · A. L. Alvarez · R. Mondragon · A. Morales
Departamento de Física, Universidad Autónoma Metropolitana Iztapalapa, Mexico, Mexico

C. Ríos · M. Alcaraz-Zubeldia · A. Diaz-Ruiz (✉)
Departamento de Neuroquímica, Instituto Nacional de Neurología y Neurocirugía Manuel Velasco Suárez S.S.A, Av. Insurgentes Sur 3877, Mexico, D.F 14269, Mexico
e-mail: adiaz@innn.edu.mx

H. Salgado-Ceballos
Unidad de Investigación Médica en Enfermedades Neurológicas, Hospital de Especialidades, Centro Médico Nacional Siglo XXI, Mexico, Mexico

H. Salgado-Ceballos
Centro de Investigación del proyecto CAMINA A.C., Mexico, Mexico

G. J. Cruz · M. G. Olayo
Departamento de Síntesis y Caracterización, Instituto Nacional de Investigaciones Nucleares, Mexico, Mexico

Introduction

After a traumatic spinal cord injury (SCI), the damaged tissue initiates a prolonged period of secondary neurodegeneration, which includes the formation of a scar and the subsequent Wallerian degeneration in the chronic phase [1]. Many reports have proposed the use of different materials for repairing the injured spinal cord tissue. Those materials include living tissue, such as stem cells implants [2], olfactory ensheathing glial cells, Schwann cells [3], trophic factors and spinal cord embryonic grafts, with the aim of facilitating the regrowth of spinal cord white matter and restoring its functionality [4]. However, up to now, they have been poorly effective.

Another approach for repairing and reconnecting the injured spinal cord tissue is the use of inert biomaterials. Among the first studies on this issue, the use of carbon filament implants to promote axonal regeneration in a model of transected rat spinal cord has been reported [5]. In that work, the authors showed the potential use of carbon filaments as an adhesion surface to give directionality for axonal regrowth. In another work, Woerly et al. [6]

implanted in the transected spinal cord of rats a biodegradable and biocompatible material synthesized with poly (N-[2-hydroxypropyl] methacrylamide) hydrogel containing an adhesive region of fibronectin Arg–Gly–Asp (NeuroGel^{TM}). The results showed angiogenesis, axonal regrowth and a decrease of necrotic processes. Another material used for the reconstruction of the injured spinal cord tissue in the same trans-section model is the poly (D,L-lactic acid), either impregnated or not with brain-derived neurotrophic factor (BDNF). Motor function was evaluated during eight weeks after surgery showing similar recovery in the control group versus implanted groups, in spite of observing cell survival and angiogenesis [7].

On another direction, the use of materials derived from pyrrole is emerging as an interesting alternative for tissue repair. Composed by heterocyclic amines, polypyrrole (PPy) is a novel electrical semiconductive material with potential use in the next generation of sensors, batteries and diodes. The electric capabilities of PPy have their origin in the conjugated double bonds participating in the heterocyclic molecules. In biological applications, the biocompatibility and biostability of PPy has been tested recently, both in vitro and in vivo [8, 9, 10]. Thus, applying its electrical and biological properties, polypyrrole can be used to create new bioengineering technologies [11] to modify cellular functions, such as migration [12], adhesion [13, 14], synthesis of DNA [15] and secretion of proteins [16] for tissue repair or for other biological functions.

The synthesis of polymeric materials derived from pyrrole is frequently performed using oxidative chemical or electrochemical methods. However, polymers obtained in this way must be carefully purified before applying them to living systems, because the impurities and contamination with entrapped solvents and catalytic reagents among the chains can have collateral effects in such systems, as increase in the inflammation response and in the degeneration processes.

The use of plasmas as ionizing agents to generate ions, electrons, photons, and molecules in excited electronic state is an alternative to promote the propagation of polymerization reactions without contaminants, instead of catalytic reagents, because in this action only participates the starting monomers and the next step products as oligomers and polymers with different molecular weight [17]. As all the chemical species involved in this kind of process are derived from the same monomer molecules, the contamination with other substances is prevented and the potential inflammation response in the implantation zone is confined practically to substances derived from the monomer combinations.

However, although the process is clean in this sense, the collisions of the accelerated particles in the electrical field imposed to the reactor with the monomer molecules and with the polymers in formation usually result in a certain degree of ramification and crosslinking in the final polymers. As a consequence, if the energy of the impacts goes far beyond the bonding energy in the molecules, they can produce fragments that participate in the chains, laterally or in the backbone, and in an extreme case, without an adequate control, the final material may result as a great network composed by fragments of the monomer molecules. Consequently, the electric, geometric and thermodynamic conditions of the plasma polymerization are critical in obtaining polymers with a high proportion of entire monomer molecules in their structure. Additionally, the synthesis can be enriched with halogenated dopants that are useful in enhancing the electric response in the final polymers.

Therefore, the combination of PPy and iodine, polymerized and doped by plasma, is studied in this work to evaluate the inflammatory response in a model of spinal cord transection in rats. In this study, we synthesized two pyrrole-derived polymers, iodine-doped polypyrrole and polypyrrole co-polymerized with polyethylene glycol (PEG), using plasma polymerization techniques. The synthesis was handled to obtain polymers with low fragmentation and a middle crosslinking to facilitate the growing of neuronal cells.

Materials and methods

Polymer synthesis

The polymeric materials used to prepare the implants were synthesized in a vacuum tubular glass reactor with an approximated volume of 1.5 L. The main tube has 9 cm of diameter and 15 cm long. The reactor has stainless steel flanges at the ends with three access ports in each flange. Through different combinations of the access ports, monomers and dopants can be introduced into the reactor to obtain homopolymers, copolymers or doped versions of both materials. In the other ports, a vacuum mechanical pump, a Pirani gauge and a liquid nitrogen gas condenser were connected to the reactor to reduce the pressure in the system and to condense the undesirable gases leaving or entering to the system. In the center of the flanges, metallic electrodes can be inserted to create a homogenous electric field in the reactor. The electrodes were made of stainless steel flat plates with 7 cm of diameter, separated 9 cm from each other. One electrode was connected to ground and the other one to a radio frequency (rf) signal by means of both, an ENI A150 RF Power Amplifier and a Wavetek Model 164 Function Generator.

The plasma was produced as electric glow discharges at 13.5 MHz, 5×10^{-2} Torr and approximated power of 18 W. The main monomer used in the polymerizations was

pyrrole (Aldrich, 99%), the dopant was iodine (Aldrich, 99.8%) and the starting polymer used in the copolymer was PEG (Aldrich). They were placed in separate reservoirs and connected to the reactor in different access. A small mass flow of each reagent required in the polymerization was introduced into the reactor by the differential pressure between the main chamber and the reagent reservoirs. The initial temperature of the monomers and dopants was approximately 25 °C. The main promoter of the chemical reactions is the formation of free radicals and ions because of the electric field imposed in the vacuum chamber. The reactions initiated in the gas phase and finished in solid phase as thin films adhered on the internal reactor surfaces. The polymerization time was 300 min for all syntheses. At the end of the reactions, the films had an approximated average thickness of 20 μm.

The polymers were separated from the internal surfaces of the reactor by applying acetone in three or four steps. This solvent swelled the films in such a way that they could be separated from the walls with a thin spatula. One homopolymer and one copolymer were synthesized, polypyrrole doped with iodine (PPy/I) and polypyrrole-polyethylene-glycol (PPy/PEG), respectively. The doping with iodine had the objective to enhance the conductive characteristics of PPy. In the first case, PPy/I, only pyrrole and iodine in gas phase entered to the reactor through two different ports. Once the reactions finished, the film was pulverized and compressed to make tablets. In the copolymer case, PPy/PEG, vapors of pyrrole and polyethylene-glycol entered, separately, to the reactor. After removing the films from the reactor, no additional preparation was made to the polymer. Both, tablets and films, were implanted in the spinal cord of the test animals.

Polymer characterization

Structure analyzed by Infrared spectroscopy (FT-IR)

The analysis of the structures formed in the polymers was obtained with a Perkin-Elmer 2000 Infrared Spectrophotometer collected directly from the films using 32 scans.

Scanning electron microscopy (SEM) and elemental analysis

The morphological characteristics of the PPy/I and PPy/PEG surfaces were observed with a Philips XL-30 Scanning Electron Microscope. The samples were covered with a thin layer of gold to increase the conductivity of the surfaces, which in consequence help to increase the magnification of the images. The microscope was coupled with a Sapphire type EDAX NXL-30 Energy Dispersive Spectroscopy (EDS) probe for elemental analysis.

Electric conductivity

The volumetric electric conductivity was calculated using the equation $\sigma = L/(R*A)$. Where σ = conductivity (S/cm), L = thickness (cm), R = resistance (Ohm), A = cross section area (cm^2). The resistance was measured perpendicular to the surface of the polymers using a two-probe device, where the sample was placed in the middle of two copper electrodes in a capacitive arrangement. The resistance of the polymers, as films or as tablets, was measured with an Otto Multimeter.

Animals

Female Long Evans rats weighing 250–300 g were used. Animals were maintained under standard laboratory conditions and had free access to food and water. Animal care and the protocols for animal use were approved by the Animals Ethics Committee of the National Institute of Neurology and Neurosurgery of Mexico.

Rats were randomly allocated into one of three groups ($n = 3$ animals per group). After pentobarbital anesthesia (50 mg/kg i.p.), all rats were subjected to a whole spinal cord section at thoracic 9 (T9) level. Under microscopic inspection, an aseptic surgery was done making an incision on the skin from the middle back and the paravertebral muscles for removing carefully two laminae (T-8 and T-9). Spinal cord tissue was exposed, the meninges were carefully cut and the spinal cord tissue was completely transected. Two groups received 10 mg of polypyrrole doped with iodine or polypyrrole-polyethylene glycol previously sterilized for 30 min. The control group did not receive any implant. All animals were treated with anti-inflammatory (5 mL/2 L into drinking water) and antibiotic drugs (200 μL of benzatinic penicillin, in one subcutaneous dose). Rats were allowed to recover from anesthesia and surgical procedures in an intensive care unit for small animals (Schoer Manufacturing CO., Kansas City, MO, USA). They were allocated in individual acrylic cages with sterile sawdust and received food and water *ad libitum*. About 24 h after transection, the absence of hindlimb movement was corroborated to assure a complete section of the spinal cord. Their intestine and bladder were handled with manual expression twice a day and visual inspection was performed for skin irritation or decubitus ulcers.

Histology and morphometric analysis

Thirty days after spinal cord trans-section, all animals were anesthetized by i.p. injection of pentobarbital, following by 1 mL of heparin, and perfused via the ascending aorta with 200 mL of cool physiological saline solution followed by 500 mL of 10% formaldehyde, using a peristaltic pump at

30 mL/min. The specimens were processed for paraffin embedment. Longitudinal sections of 10 μm thick were serially obtained, including the lesion area and neighboring tissues. All the sections were stained with hematoxylin and eosin for histological and morphometric analysis, luxol fast blue was used for myelin fibers, and Masson trichromic staining for collagen.

Sample images were obtained using a computerized system equipped with an IM 1000 software and a 300 FX digital camera. Pathologic analysis was performed with an Image Database V.4.01 (Leica) and a CCD-IRIS Sony camera, using morphometric assessment.

Damaged tissue was identified as scaring tissue surrounding cavities and loss of normal tissue architecture.

The spared spinal cord tissue was measured on an area of 2,057 mm^2 surrounding the lesion; only one cut was considered for the analysis. In order to have comparable area for evaluation, the ependymus was taken as the point of reference [18].

Immunohistochemistry

To determine the identity of cells located at the area of lesion, all groups were examined using specific anti-bodies to identify macrophages (MAC) and astroglial cells (GFAP).

The animals ($n = 3$) were perfused through the heart with buffered saline, followed by 10% formaldehyde. The spinal cord tissue from T8 to T10 segments was removed and stored in formaldehyde. The tissue was sectioned on a freezing microtome at 10 μm.

Some series of sections were processed for GFAP and MAC visualization. The sections were first incubated in 3% normal sheep serum in TBS (50 mM TRIS buffer, pH 7.2, containing 0.9% saline solution) for 3 h at room temperature to block the non-specific binding, followed by incubation with monoclonal anti-GFAP (Zymed, 1:250) and anti-MAC (Immunotech, 1:150) for 36 h at 4 °C. After washing three times (15 min each) with TBS, the sections were incubated in biotinylated anti-mouse antibody, and then with streptavidin conjugated to HRP (horse-radish peroxidase, 1:400). The anti-bodies were visualized with diaminobenzidine (DAB).

Examination of the microscopic specimens was done by a blind observer unaware of the specific treatment received by the animals.

Statistical analysis

Results of spared spinal cord tissue were statistically analyzed by one-way ANOVA followed by Dunnett's test, after testing for homogeneity of variances. All analyses were performed by using the SPSS 13.0 software.

Results

Elemental analysis

Table 1 presents the elemental analysis obtained from the polymers using EDS techniques. The elements analyzed were Carbon, Nitrogen, Oxygen and Iodine. Carbon and Nitrogen constitute the structure of both monomers used in this work. Oxygen is part of the ethylene glycol structure, but does not participate in that of pyrrole. So, the Oxygen fraction found in PPy/PEG originates from both, the structure and the oxidation of the polymer coming from the reaction of the last free living radicals in the polymers with the atmospheric oxygen, at the end of the reactions.

Iodine doping was applied only to the PPy/I polymers, that is why it does not appear in PPy/PEG. The fraction of iodine in PPy/I is almost half of the total polymer weight. Some of the atoms could be chemically linked with the polymers and others could be trapped among the chains without being linked to a specific site in the structure. Although the amount of iodine is high in weight, in terms of atoms it would represent approximately one iodine atom for each two monomer rings in the final structure of PPy/I. This estimation can be done taking in consideration that each nitrogen atom represent one pyrrole ring in the polymers.

FT-IR analysis

The spectra in Fig. 1 contain the IR absorptions of PPy/I (A) and PPy/PEG (B). The spectra are composed mainly with three wide absorption bands. The first one is located in the 2,500–3,800 cm^{-1} region and can be associated with the complex C–H, N–H and O–H interactions in the polymers. This region is narrower in PPy/I because the O–H interactions in this polymer originates only from the final atmospheric oxidation. On the other hand, PPy/PEG has two sources of O–H bonds, from the ethylene glycol structure and from the atmospheric oxidation. The absorption centered between 2,946 and 2,932 cm^{-1}, included in both polymers, can be assigned to the C–H aliphatic groups. This absorption suggests the presence of pyrrole fragments included in the macromolecules. The vibration in 2,220 cm^{-1} corresponds to nitrile groups, C≡N,

Table 1 Elemental composition in % weight of PPy/I and PPy/PEG

Element	PPy/I	PPy/PEG
Carbon	33.6	65.3
Nitrogen	12.1	24.0
Oxygen	4.9	10.7
Iodine	49.4	0
Total	100.0	100.0

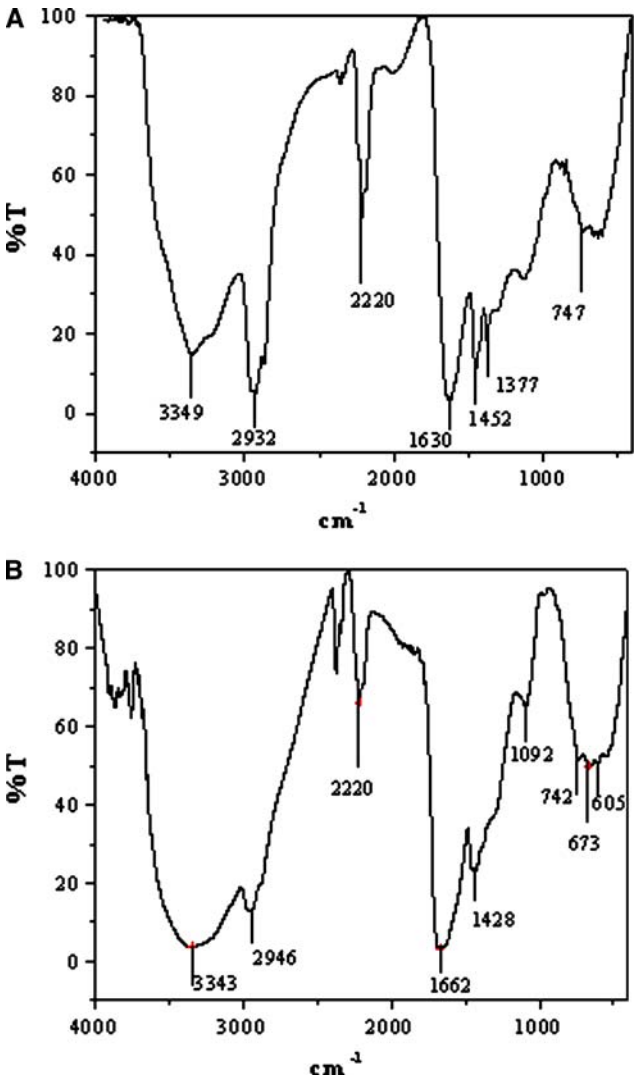

Fig. 1 (**A**) FT-IR spectrum of polypyrrole doped with iodine, (**B**) FT-IR spectrum of co-polymer of polypyrrole-polyethylene glycol

and suggests also the breakage of some monomer rings and the partial nitridation of the fragments. The nitrogen involved in this process comes from the pyrrole molecules and from the final atmospheric interaction. This absorption is more intense in PPy/I.

The second wide absorption is located in the 1,000–1,800 cm^{-1} band. Between 1,600 and 1,800 cm^{-1}, the presence of C–N, C=C and C=0 groups can be found. The 1,630 and 1,662 cm^{-1} peaks belong to amines and carbonyl groups, respectively. In PPy/PEG, the main peak in this band is closer to 1,700 cm^{-1} because of the oxygen influence in PEG molecules. However, in PPy/I, this band is closer to 1,600, where the amines in the heterocycles predominates.

The third wide absorption band is positioned in the 400–800 cm^{-1} interval. The substitutions in pyrrole rings, associated with the growing of the polymers and with the partial ramification and crosslinking among the chains, can be found in this band. This complex absorption indicates the networking in the polymers.

Morphology analysis

The PPy/I surface (Fig. 2A) has the characteristic agglomerates of the PPy synthesized by plasma formed by spheres of 5–10 μm diameter [17]. The roughness is important, because an increase in this characteristic gives more superficial area where the cells can interact with the polymers. In contrast, the PPy/PEG copolymer (Fig. 2B) has a rather smooth surface with a flaked appearance.

Electric conductivity

The electrical resistance of the PPy/I tablet was 1.3 MΩ at low relative humidity (30%) and its associated conductivity was 21 nS/cm. The PPy/PEG copolymer resistance, as films, was higher than 2 GΩ; which means conductivity lower than 10^{-12} S/cm. It has been reported that the conductivity of some polymers and copolymers constituted by pyrrole and polymerized and doped by plasma with

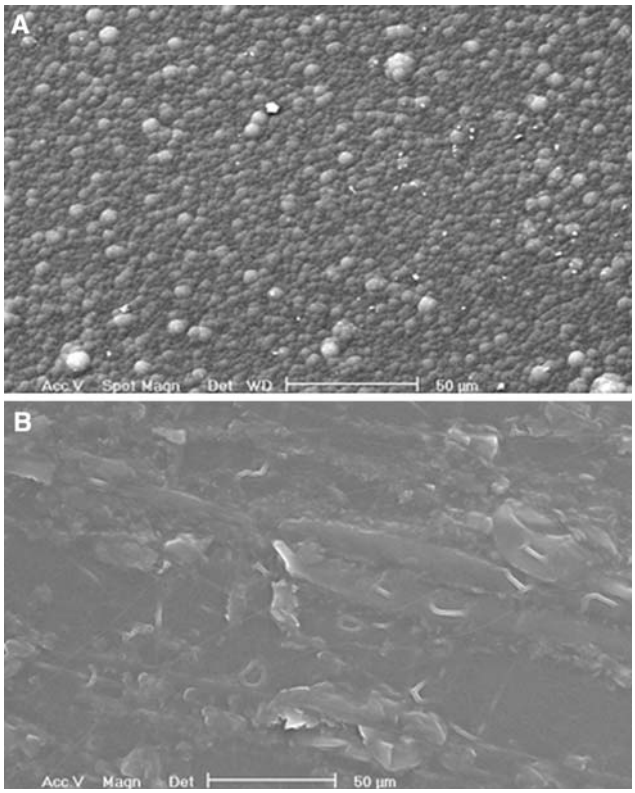

Fig. 2 Representative SEM micrographs of the polymers obtained with a Philips XL-30 Scanning Electron Microscopy. (**A**) The surface of polypyrrole doped with iodine (**A**) has the characteristic agglomerates formed by spheres of a 5–10 μm diameter. In contrast, co-polymer of polypyrrole-polyethylene glycol (**B**) has a flaked structure. Bar represents 50 μm

iodine, as those used in this work, follows an ohmic behavior [19], but increases several orders of magnitude at high relative humidity (>60%) [17, 19, 20]. This point is important, because once implanted in the spinal cord of the test animals, the polymers are surrounded by water and body fluids, which most surely increase the conductivity.

Survival

The use of implants of PPy/I and PPy/PEG showed no deleterious effects on the survival of animals, as all animals recovered and survived until the time of killing. In the three groups of treatment, some animals showed hematuria for the first 72 h, without infections. Animals also presented light skin irritations.

Histological description of the spinal cord

Thirty days after the implants, the animals were killed to analyze the integration of the two materials into the spinal cord tissue. Morphological examinations of spinal cord tissue of all animals implanted or not with PPy/I and PPy/PEG are shown in Fig. 3. The panels A, C and E show panoramic images of the complete section zone of spinal cord with or without implant, and the tissue interface at 4 weeks after the implants stained with luxol fast blue technique (B, D and F).

In the tissue from animals receiving the implants, a good integration of materials was observed with a concomitant cell proliferation (Fig. 3 panels D and F). In the group implanted with PPy/I there are few cavities in the spinal cord interface**.** The group implanted with PPy/PEG presents cysts into implant zone, but not in the peripheral area, showing preservation of the remaining tissue (Fig. 3, panel F). Microphotographs from control group animals (only transection) showed cysts of variable sizes and the lesion zone appears to extend to the adjacent white and gray matters, (Fig. 3, panel B). The presence of inflammatory response was still observed 4 weeks after spinal cord transaction, using the hematoxylin/eosin staining. Inflammation was observed in the white and gray matter adjacent tissue, and in the implant zone, although, this response was higher in the control group, after quantitative analysis with morphological criteria [18] (Fig. 4). The presence of fibroblast and collagen proliferation was observed in both, the lesion and the implant zone (Fig. 5 panels B, E and H respectively) as well as, in the adjacent zone of spinal cord

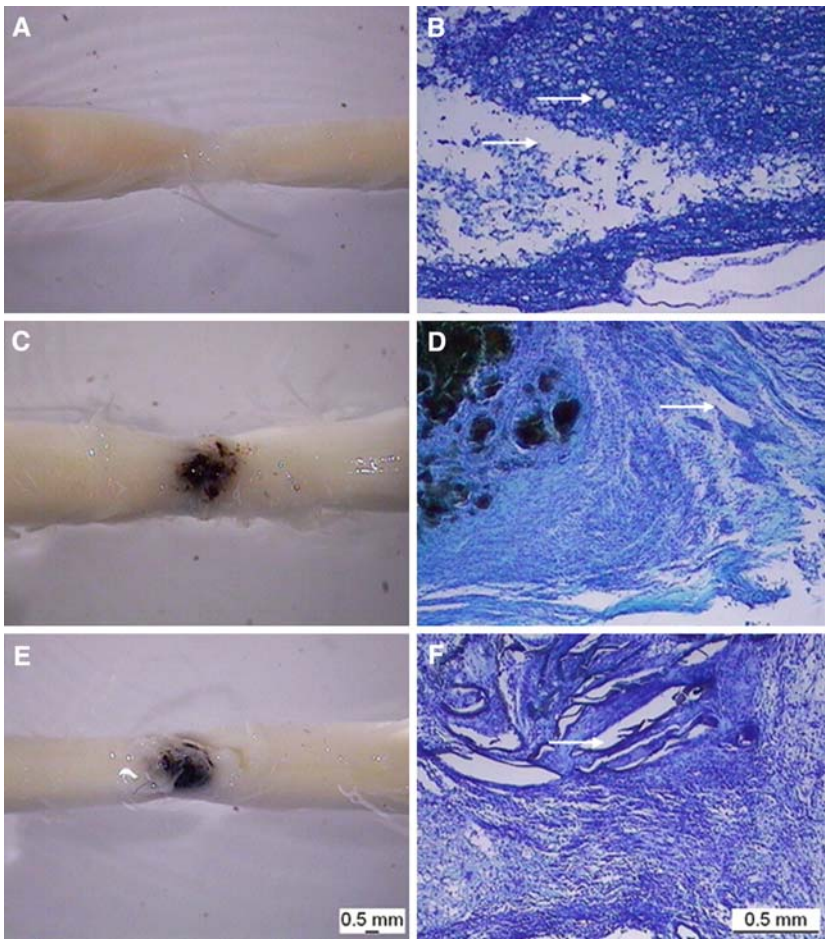

Fig. 3 Left-hand side photographs: spinal cord showing the zone of transection. Control animal, without implant (**A**). Animal implanted with polypyrrole doped with iodine (**C**); or polypyrrole and co-polymerized with polyethylene glycol (**E**). Right-hand photographs of horizontal spinal cord interface area: Control animal (**B**), polypyrrole doped with iodine implanted animal (**D**) and polypyrrole and co-polymerized with polyethylene glycol implanted animal (**F**). Arrows show cysts of variable sizes and shapes. Luxol fast blue stain

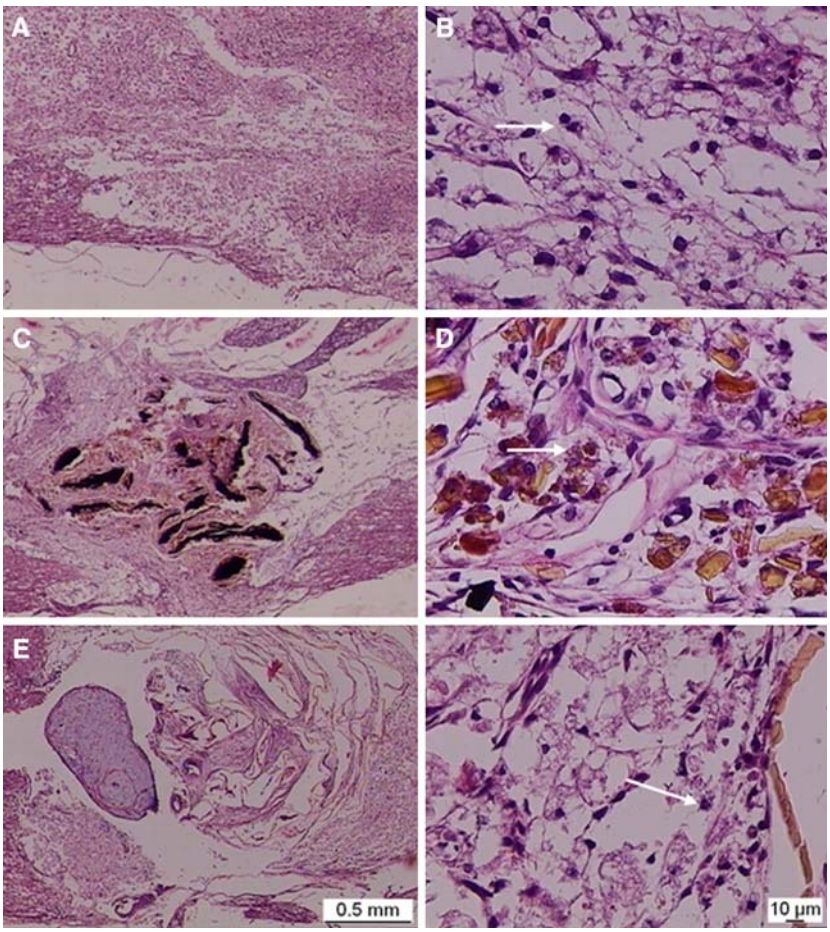

Fig. 4 Representative microphotographs of horizontal sections of spinal cord that show the zone of transection without implant (control group, **A**) and implant of polypyrrole doped with iodine (**C**) or polypyrrole and co-polymerized with polyethylene glycol (**E**). **B**, **D** and **F** amplified areas of **A**, **C** and **E** respectively. Arrows show inflammatory cells. Hematoxylin/eosin stain

tissue (Fig. 5 panels C, F and I).The control group showed less collagen in the lesion epicenter as compared to the groups receiving the implants with PPy/I and PPy/PEG. In all cases, the transition zone (area among spinal cord tissue and implant zone) was examined. The neighboring spinal cord tissue appeared less damaged in the transplanted rats than in the non-implanted animals.

Analysis of spared spinal cord tissue at epicenter

The amount of spared spinal cord tissue was quantified for each group and it is shown in Fig. 6. The mean percentage of spinal cord spared tissue in the 2057 mm^2 analyzed area in control group was 14.3%, while in the groups implanted with PPy/I and PEG the means were 32.5 and 35.3% ($p = 0.007$, one way ANOVA, followed by Dunnett's test, $p < 0.016$ and 0.006, respectively) for control versus PPy/I and PEG groups, respectively.

Immunohistochemistry

All the experimental groups showed intense reaction as defined by MAC infiltration or glial reaction (GFAP). Cellular immunoreactivity was found similar between the control group (Fig. 7A and D) and that of animals implanted with either with PPy/PGE (Fig. 7-B and E) or PPy/I, using MAC and GFAP immunostaining.

Discussion

The present study shows a good integration of the polymers obtained by plasma polymerization of polypyrrole and PEG into the transected spinal cord tissue, as well as an increased cell proliferation and sparing of the remaining tissue. The physico-chemical characteristics of the materials employed here are important, since both materials are non-biodegradable and have potential to transport electric charges. The application of these plasma polymers is a novelty in this study, because the materials were synthesized without chemical reagents that could increase the inflammatory response in living tissues.

Plasma discharges using direct current (dc) allow high currents between electrodes, which easily lead to the degradation of the labile species participating in the reactions, as the heteroaromatic cycles composed by polypyrroles.

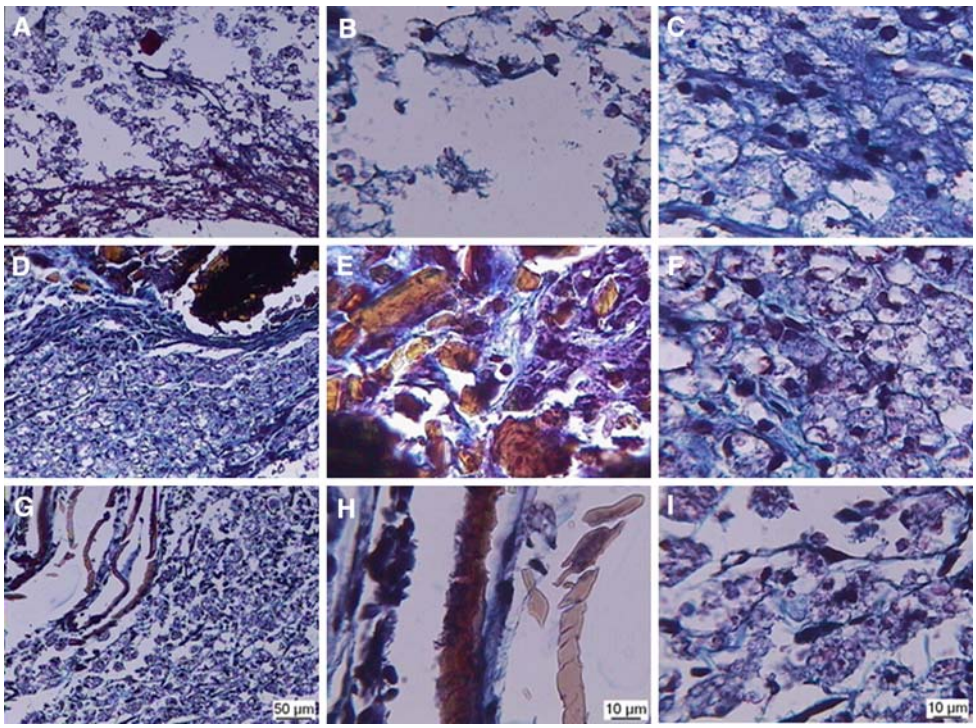

Fig. 5 Representative microphotographs of horizontal sections of spinal cord that showed the zone of complete transection of control, without implant rats (**A**) and implant zone of polypyrrole doped with iodine (**D**) or polypyrrole co-polymerized with polyethylene glycol (**G**). Amplified implant area (**B**, **E** and **H**, respectively) and adjacent zone (**C**, **F** and **I**). Masson trichrome stain

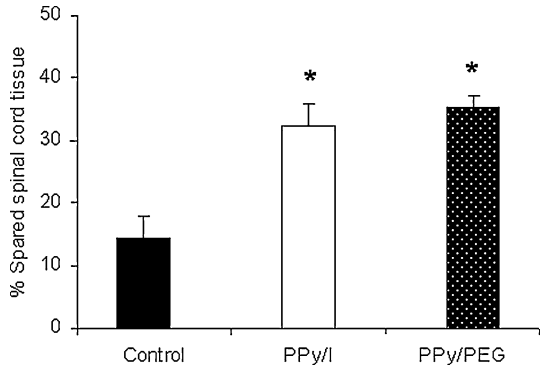

Fig. 6 Area of spared spinal cord tissue at level from epicenter of lesion. Results of morphometric measurements are expressed as percentage of spared spinal cord tissue of three animals per group. Control: only transection spinal cord, PPy/I: transection spinal cord plus polypyrrole doped with iodine, PPy/PEG: transection spinal cord plus co-polymer of polypyrrole-polyethylene glycol. *Different from control group ($p = 0.007$ one way ANOVA, followed by Dunnett's test, $p < 0.016$ and 0.006, respectively)

Radiofrequency plasma glow discharges can be produced with particle energies in the range of the organic chemical bonds, allowing the synthesis of complex organic compounds. This is the reason why this kind of discharges is used in many organic polymerizations. On the other hand, higher frequencies usually need higher energies to produce the plasma environment; in such a way that microwave discharges are used mainly in obtaining inorganic compounds. However, even in the case of rf plasmas, the electrodes used in the resistive plasma coupling accelerate the ionized particles so high in the neighborhood, that the polymers formed on the nearest surfaces usually have more fragmentation and crosslinking than those formed in other surfaces of the reactor. Nevertheless, crosslinking in the polymers can have advantages from a biological point of view, because the network produced by the plasma can serve as a polarized three-dimensional support where the tissue cells can grow promoted by the electric interaction between the neuronal cells and the network. Therefore, crosslinking could be additionally induced to increase the growing of the neuronal cells. However, an undesirable consequence in doing that is that the networked polymers alter the electric configuration among the chains resulting in reduced electric conductivity.

In this point the dopants appear, increasing the electric conductivity in the materials by adding atoms with lower or higher concentration of electrons that work as polarized sites along the chains. However, in biological systems, the dopants should not increase the inflammatory response in the tissues. Among others, one of the dopants that have been successfully tested in increasing the electric conductivity in PPy is iodine; and this dopant has also been used as antiseptic in the treatment of superficially damaged skin tissues since long time ago.

Nevertheless, it is convenient to mention that the plasma doping has different characteristics from the typical physicochemical doping. Depending on the kinetic energy of the plasma particles, in plasma doping, chemical bonds between the polymer chains and the dopants might appear

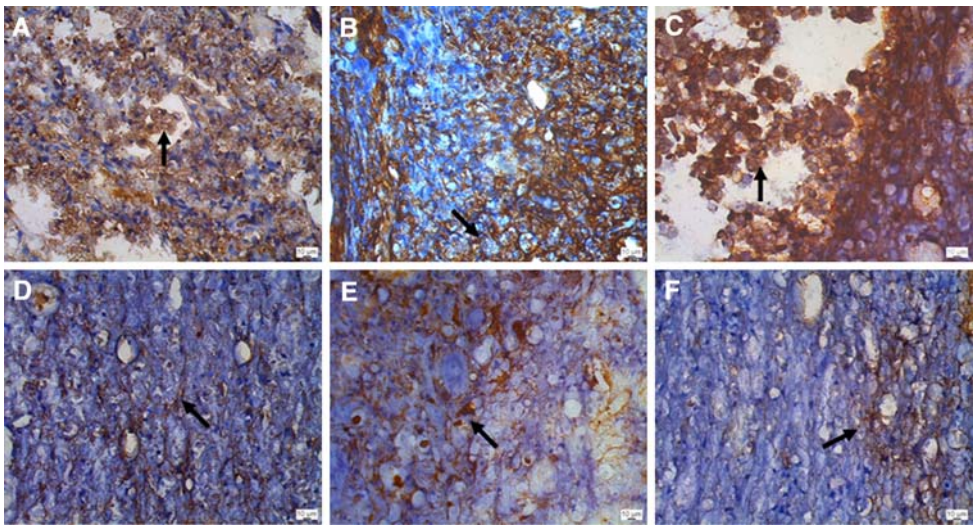

Fig. 7 Distribution of macrophages identified by MAC monoclonal antibody. Control group (**A**), group implanted with polypyrrole doped with iodine (**B**) and polypyrrole co-polymerized with polyethylene glycol (**C**). Distribution of astrocytes identified with GFAP anti-body. Control group (**D**), group implanted with polypyrrole doped with iodine (**E**) and polypyrrole co-polymerized with polyethylene glycol (**F**). Arrows show macrophages and astrocytes

transforming the predominantly physical process in a combination of physical and chemical ones[17]. So, polypyrrole obtained and doped by plasma with iodine, contains iodine atoms linked physically and chemically in the structure, which changes the physico-chemical properties of the polymer producing a semiconductive material with affinity to water [17]. Because of this affinity, the PPy/I-Water system can increase its electric conductivity up to seven magnitude orders respect to the non-doped PPy-Water system. This characteristic is very important in biological systems, because water is an essential component in tissues and other living systems.

Acting on spinal cord tissue, the polymeric materials applied in this work are probably diminishing the inflammatory response after injury, a mechanism frequently associated to a poor outcome after the implant of biomaterials [21]. Tissue tolerability to the materials employed was also showed, as no adverse reaction was observed after polymer implant, in terms of infections or implant rejection, and a similar response of MAC and glial cells in all groups.

The use of biomaterials derived from pyrrole may be a good alternative for the treatment of injured spinal cord. Similar polymers obtained by chemical techniques have been tested both in vitro and in vivo in neuronal cells and central nervous system, respectively [22, 23]. Tissue culture polystyrene dishes covered by polypyrrole showed enhanced cell adhesion and proliferation of mesenchymal stem cells and neural cells [24, 22]. The use of polypyrrole implants into the brain in vivo have also been used as a tool to provide a conductive substrate in order to promote neural interaction [23].

Biodegradable materials made of lactic poly(D,L-acid) (PLA50) with a co-polymer of high molecular weight of lactic poly(L-acid) to 10% of lactic poly(L-acid) (PLA100/10), were also implanted before in the transected spinal cord of rats [25]. Some other biodegradable materials have also been employed as implants after transection of spinal cord, such as: poly(D,L-lactide), modified with 10 wt% of the poly(ethylene oxide)-block-poly(D,L-lactide) copolymers, loaded or not with acid fibroblast growth factor [26]; poly-beta-hydroxybutyrate (PHB) fibers, plus alginate hydrogel, fibronectin and Schwann cells [27]. However, one of the main limitations for the use of biodegradable synthetic materials to repair spinal cord is the inflammatory response triggered by degradation of biomaterials, leading to progressive tissue loss and cystic cavitation [28].

The materials tested in this study showed a better response from host tissue, rendering reduced cystic cavitation and tissue sparing, two conditions reflecting good tolerability by central nervous system to the biomaterials employed.

Conclusion

The non-biodegradable semiconductor biomaterials derived from pyrrole, obtained by plasma polymerization, showed good compatibility after implant into the transectioned spinal cord tissue and produced improved cell proliferation and increased tissue sparing. Therefore, iodine-doped polypyrrole and polypyrrole co-polymerized with PEG could be considered as new biomaterials that may be used in the bioengineering to repair spinal cord damage.

Acknowledgments We thank to Dr. Jorge Guevara, Dr. Gabriel Guizar-Sahagún and Tec. Noemi Gelista Herrera from the National Institute of Neurology and Neurosurgery of Mexico, for their valuable assistance in the analyzing and capture of images. This work was supported by CONACyT grant No. 47467.

References

1. M. S. BEATTIE, G. E. HERMANN, R. C. ROGERS and J. C. BRESNAHAN, *Prog. Brain Res.* **137** (2002) 37
2. S. XIANG, W. PAN and A. J. KASTIN, *Curr. Pharm. Des.* **11** (2005) 1267
3. D. J. BARAKAT, S. M. GAGLANI, S. R. NERAVETLA, A. R. SANCHEZ, C. M. ANDRADE, Y. PRESSMAN, R. PUZIS, M. S. GARG, M. B. BUNGE and D. D. PEARSE, *Cell Transplant.* **14** (2005) 225
4. M. NAKAMURA, H. OKANO, Y. TOYAMA, H. N. DAI, T. P. FINN and B. S. BREGMAN, *J. Neurosci. Res.* **81** (2005) 457
5. T. KHAN, M. DAUZVARDIS and S. SAYERS, *Brain Res.* **541** (1991) 139
6. S. WOERLY, E. PINET, L. de ROBERTIS, D. van DIEP and M. BOUSMINA, *Biomaterials* **22** (2001) 1095
7. C. M. PATIST, M. B. MULDER, S. E. GAUTIER, V. MAQUET, R. JEROME and M. OUDEGA, *Biomaterials* **25** (2004) 1569
8. Z. ZHANG, R. ROY, F. J. DUGRE, D. TESSIER and L. H. DAO, *J. Biomed. Mater. Res.* **57** (2001) 63
9. X. JIANG, D. TESSIER, L. H. DAO and Z. ZHANG, *J. Biomed. Mater. Res.* **15** (2002) 62
10. G. SHI, M. ROUABHIA, Z. WANG, L. H. DAO and Z. ZHANG, *Biomaterials* **25** (2004) 2477
11. J. WANG, K. G. NEOH and E. T. KANG, *Thin Solid Films* **446** (2004) 205
12. X. LI and J. KOLEGA, *J. Vasc. Res.* **39** (2002) 391
13. C. E. PULLAR, R. R. ISSEROFF and R. NUCCITELLI, *Cell Motil. Cytoskeleton* **50** (2001) 207
14. M. J. BROWN and L. M. LOEW, *J. Cell Biol.* **127** (1994) 117
15. H. OZAWA, E. ABE, Y. SHIBASAKI, T. FUKUHARA and T. SUDA, *J. Cell Physiol.* **138** (1989) 477
16. V. A. MCBAIN, J. V. FORRESTER and C. D. MCCAIG, *Invest. Ophthalmol. Vis. Sci.* **44** (2003) 540
17. G. J. CRUZ, J. MORALES and R. OLAYO, *Thin solid films* **342** (1999) 119
18. G. GUIZAR-SAHAGUN, I. GRIJALVA, I. MADRAZO, R. FRANCO.BOURLAND, H. SALGADO-CEBALLOS, A. IBARRA and J. LARRIVA-SAHD, *Rest. Neurol. Neurosci.* **7** (1994) 61
19. J. MORALES, M. G. OLAYO, G. J. CRUZ, M. M. CASTILLO-ORTEGA and R. OLAYO, *J. Polymer Science Part B: Polymer Physics* **38** (2000) 3247
20. J. MORALES, M. G. OLAYO, G. J. CRUZ and R. OLAYO, *J. Appl. Poly. Sci.* **85** (2002) 263
21. R. GONZALEZ, J. GLASER, M. T. LIU, T. E. LANE and H. S. KEIRSTEAD, *Exp. Neurol.* **184** (2003) 456
22. S. LAKARD, G. HERLEM, N. VALLES-VILLAREAL, G. MICHEL, A. PROPPER, T. GHARBI and B. FAHYS, *Biosens Bioelectron* **20** (2005) 1946
23. P. M. GEORGE, A. W. LYCKMAN, D. A. LAVAN, A. HEGDE, Y. LEUNG, R. AVASARE, C. TESTA, P. M. ALEXANDER, R. LANGER and M. SUR, *Biomaterials* **26** (2005) 3511
24. H. CASTANO, E. A. O'REAR, P. S. MCFETRIDGE and V. I. SIKAVITSAS, *Macromol. Biosci.* **4** (2004) 785
25. M. OUDEGA, S. E. GAUTIER, P. CHAPON, M. FRAGOSO, M. L. BATES, J. M. PAREL and M. B. BUNGE, *Biomaterials* **22** (2001) 1125
26. V. MAQUET, D. MARTIN, F. SCHOLTES, R. FRANZEN, J. SCHOENEN, G. MOONEN and R. JÉRÔME, *Biomaterials* **22** (2001) 1137
27. L. N. NOVIKOV, L. N. NOVIKOVA, A. MOSAHEBI, M. WIBERG, G. TERENGHI and J. O. KELLERTH, *Biomaterials* **23** (2002) 3369
28. M. S. BEATTIE, *Trends. Mol. Med.* **10** (2004) 580